Atmos. Chem. Phys., 7, 5263–5274, 2007
www.atmos-chem-phys.net/7/5263/2007/

Atmospheric Chemistry and Physics

Inferring thermodynamic properties from CCN activation experiments: single-component and binary aerosols

L. T. Padró[1], A. Asa-Awuku[1], R. Morrison[1,*], and A. Nenes[1,2]

[1]School of Chemical and Biomolecular Engineering, Georgia Institute of Technology, Atlanta, GA, 30332, USA
[2]School of Earth and Atmospheric Sciences, Georgia Institute of Technology, Atlanta, GA, 30332, USA
[*]now at: Department of Chemical Engineering, University of Texas, Austin, TX, 78712, USA

Received: 12 February 2007 – Published in Atmos. Chem. Phys. Discuss.: 15 March 2007
Revised: 20 September 2007 – Accepted: 1 October 2007 – Published: 12 October 2007

Abstract. This study presents a new method, Köhler Theory Analysis (KTA), to infer the molar volume and solubility of organic aerosol constituents. The method is based on measurements of surface tension, chemical composition, and CCN activity coupled with Köhler theory. KTA is evaluated by inferring the molar volume of six known organics (four dicarboxylic acids, one amino acid, and one sugar) in pure form and in mixtures with ammonium sulfate ($(NH_4)_2SO_4$). The average error in inferred molar volumes are to within 18% of their expected value for organic fractions between 50 and 90%. This suggests that KTA is a potentially powerful tool for determining the CCN characteristic of ambient water soluble organic carbon (WSOC), providing physically-based constraints for aerosol-cloud interaction parameterizations.

1 Introduction

It is well accepted that atmospheric aerosols affect climate directly by reflecting incoming solar radiation (IPCC, 2001) and indirectly through their role as cloud condensation nuclei (CCN) (Twomey, 1977; Albrecht, 1989; IPCC, 2001). Understanding the cloud droplet formation potential of aerosols is a requirement for predicting their impacts on clouds, and currently is a large source of uncertainty in climate change predictions. Aerosols in the atmosphere are composed of inorganic and organic compounds which influence their ability to act as CCN. Past studies have shown that particulate matter composed of water-soluble inorganic salts and low molecular weight dicarboxylic organic acids can act as efficient CCN (Cruz and Pandis, 1997; Facchini et al., 1999a; Giebl et al., 2002; Raymond and Pandis, 2002; Kumar et al., 2003) which is adequately modeled by Köhler theory (Köhler, 1936). Köhler theory can also predict, with appropriate modifications, the CCN activity of higher molecular weight organic compounds (such as some polycarboxylic acids, fatty acids, alcohols, and amines (Raymond and Pandis, 2002; Hartz et al., 2006)) which constitute a significant fraction of the water soluble species (Zappoli et al., 1999; Decesari et al., 2000; Broekhuizen et al., 2006; Sullivan and Weber, 2006a, b).

Organics primarily influence CCN activity by contributing solute and depressing surface tension; both affect the equilibrium water vapor pressure needed for droplet activation (Shulman et al., 1996; Facchini et al., 1999b; IPCC, 2001; Feingold and Chuang, 2002; Nenes et al., 2002; Kanakidou et al., 2005). A modified version of Köhler theory, incorporating both limited solute solubility and surface tension depression for slightly soluble species was first presented by Shulman et al. (1996); subsequently, Facchini et al. (2000) showed that the surface tension depression could be important for water soluble organic carbon (WSOC) typically found in polluted environments. Decesari et al. (2000) found that WSOC is composed of a complex mixture of neutral and acidic polar compounds, the most hydrophobic of which are responsible for the surface tension depression. Organics may also impact the droplet growth kinetics of CCN (Feingold and Chuang, 2002; Nenes et al., 2002), but this is not the subject of the current study.

Apart from surface tension depression, the solute thermodynamic properties such as the molar volume (molar mass over density), solubility, and effective van't Hoff factor affect CCN activity. Such parameters are very difficult to compute for ambient aerosols, as they are a complex and highly variable mixture of organic/inorganic compounds. As challenging as it may be, this characterization is required to establish

Correspondence to: A. Nenes
(nenes@eas.gatech.edu)

a physically-based link between organic aerosol and cloud droplet formation. In this work, we propose and develop a new methodology called Köhler Theory Analysis (KTA) to address this need. KTA is based on using Köhler theory to infer molar volume and solubility from CCN activation measurements (measurements of chemical composition and surface tension may be required as well). In subsequent sections, we present the theoretical basis of KTA and its application. KTA is then evaluated by inferring the molar volume of six known organics (four dicarboxylic acids, one amino acid, and one sugar) in pure form and in mixtures with $(NH_4)_2SO_4$.

2 Köhler theory analysis

2.1 Single component CCN

Köhler theory is based on thermodynamic equilibrium arguments and computes the equilibrium saturation ratio, S, of a wet particle of diameter, D_p, from the contribution of curvature (Kelvin) and solute (Raoult) terms,

$$S = \frac{P^w}{P^{\text{sat}}_{\text{flat,w}}} = \exp\left(\frac{A}{D_p} - \frac{\upsilon\phi n_s}{n_w}\right) \tag{1}$$

where $A = \frac{4M_w\sigma}{RT\rho_w}$, P^w is the droplet water vapor pressure, $P^{\text{sat}}_{\text{flat,w}}$ is the saturation water vapor pressure over a flat surface at the temperature T, M_w is the molar mass of water, σ is the droplet surface tension at the point of activation, R is the ideal gas constant, ρ_w is the density of water, υ is the effective van't Hoff factor of the solute, ϕ is the osmotic coefficient, n_s is the moles of solute, and n_w is the moles of water contained in the particle. The Kelvin or curvature effect (A term) is dependent on the droplet surface tension and tends to increase the saturation ratio; the Raoult (or solute) effect tends to decrease the saturation ratio by contribution of solute to the growing droplet.

If the CCN is composed of a single component that completely dissolves in water and is dilute (ϕ=1), Eq. (1) reduces to the well known Köhler curve (Seinfeld and Pandis, 1998),

$$\frac{P^w}{P^{\text{sat}}_{\text{flat,w}}} = \exp\left(\frac{A}{D_p} - \frac{B}{D_p^3}\right) \tag{2}$$

where:

$$B = \frac{6n_s M_w \upsilon}{\pi\rho_w} \tag{3}$$

The maximum ("critical") saturation ratio of the Köhler curve is given by (Seinfeld and Pandis, 1998)

$$S_c = \exp\left(\frac{4A^3}{27B}\right)^{1/2} \tag{4}$$

S_c corresponds to the minimum level of water vapor saturation required for a CCN to develop into a cloud droplet. Since critical saturations are always higher than unity, the critical supersaturation, s_c (defined as $S_c - 1$) is often used in its place. For each s_c, there is a characteristic dry diameter (d_{pc}), above which all particles with similar composition activate into cloud droplets.

2.2 Multi-component CCN

If the aerosol is composed of more than one component (e.g., organic and inorganic), Köhler theory can still be applied with appropriate modifications to the Raoult (solute) term (e.g., Raymond and Pandis, 2003; Bilde and Svenningsson, 2004):

$$\begin{aligned} B = \sum_i B_i &= \sum_i \left(\frac{\rho_i}{\rho_w}\right)\left(\frac{M_w}{M_i}\right)\varepsilon_i \upsilon_i d^3 \\ &= d^3\left(\frac{M_w}{\rho_w}\right)\sum_i \left(\frac{\rho_i}{M_i}\right)\varepsilon_i \upsilon_i \end{aligned} \tag{5}$$

where d is the dry diameter of the CCN, and ρ_i, ε_i, υ_i, and M_i are the density, volume fraction, effective van't Hoff factor and molar mass of the solute i, respectively. ε_i is related to the mass fraction of i, m_i, as:

$$\varepsilon_i = \frac{m_i / \rho_i}{\sum_i m_i / \rho_i} \tag{6}$$

where m_i is assumed to be known from measurements. For a single component aerosol, ε_i=1, and Eq. (5) reduces to Eq. (3).

2.3 Köhler theory analysis: inferring molar volume

If the CCN is a mixture of completely soluble organic and inorganic material then theory gives,

$$\begin{aligned} s_c &= \left(\frac{256M_w^3\sigma^3}{27R^3T^3\rho_w^3}\right)^{1/2}\left[\sum_i \left(\frac{\rho_w}{M_w}\right)\left(\frac{M_i}{\rho_i}\right)\frac{1}{\varepsilon_i\upsilon_i}\right]^{1/2} d^{-3/2} \\ &= \omega d^{-3/2} \end{aligned} \tag{7}$$

where

$$\omega = \left(\frac{256M_w^3\sigma^3}{27R^3T^3\rho_w^3}\right)^{1/2}\left[\sum_i \left(\frac{\rho_w}{M_w}\right)\left(\frac{M_i}{\rho_i}\right)\frac{1}{\varepsilon_i\upsilon_i}\right]^{1/2} \tag{8}$$

is termed the "Fitted CCN Activity" (FICA) factor. If FICA is known from CCN activity measurements, the molar volume of the water soluble organic carbon component, $\frac{M_j}{\rho_j}$, can be inferred if the surface tension at the point of activation, organic and inorganic fraction as well as the effective van't Hoff factor of the components present are known. $\frac{M_j}{\rho_j}$ can be explicitly solved by rearranging Eq. (8) as follows:

$$\frac{M_j}{\rho_j} = \frac{\varepsilon_j\upsilon_j}{\frac{256}{27}\left(\frac{M_w}{\rho_w}\right)^2\left(\frac{1}{RT}\right)^3\sigma^3\omega^{-2} - \sum_{i\neq j}\frac{\rho_i}{M_i}\varepsilon_i\upsilon_i} \tag{9}$$

where j is used to denote the organic component of the aerosol and i refers to all compounds (organic, inorganic, except "j") present in the particle.

Equation (9) is the basis of Köhler Theory Analysis, and can be applied in a variety of ways, depending on the amount of inorganic and surfactants present (which affect the scaling of CCN critical supersaturation with dry diameter). If CCN are composed of an internal mixture of a completely soluble electrolyte with insoluble material, and their proportion does not change with size, Köhler theory states that the critical supersaturation of CCN scales with $d^{-3/2}$ (this scaling relationship can change of course if partially soluble substances are present, if composition varies with size, or if strong surfactants are present). Based on the above, Eq. (9) can be applied as follows:

a) If there are no strong surfactants present (i.e., surface tension of the CCN at the point of activation does not depend on the solute concentration since it essentially stays constant): ω does not depend on d (surface tension depends on concentration and therefore size) and its value can be determined by a power law fit to the CCN activation curves. Equation (9) is then applied to infer the WSOC molar volume, given that the volume fractions and composition of organics and inorganic presents are known. This method is applied primarily in this study.

b) However if there are strong surfactants present (i.e., surface tension of the CCN at the point of activation is strongly affected by the solute concentration), the critical supersaturation – dry particle diameter curve can be divided into two regions: one in which the CCN is dilute at the point of activation and surface tension does not vary much (low critical supersaturation, or, large dry particle diameters), and, one which surface tension varies substantially (high critical supersaturation, or, small dry particle diameters). For each regime, Eq. (9) can be applied differently as follows:

b_1) Dilute regime: Since the CCN is dilute at the point of activation at low supersaturations (i.e., ω does not depend on d since surface tension is relatively constant), hence method "a" can be applied for this range. The appropriate supersaturation range can be determined by examining the slope (d exponent) of the activation curves.

b_2) Concentrated regime: In this case, the CCN can not be assumed to be dilute at the point of activation (high supersaturations), the WSOC molar volume is inferred at each supersaturation (dry diameter), using the relevant value of surface tension. We then compute the average molar volume over the range of supersaturations considered.

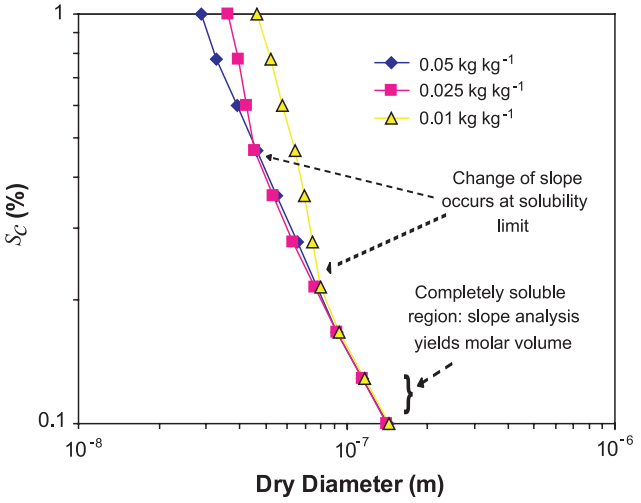

Fig. 1. Example on how CCN activation experiments can be used to infer the solubility of compounds.

2.4 Molar volume uncertainty analysis

The uncertainty in inferred organic molar volume, $\Delta\left(\frac{M_j}{\rho_j}\right)$, can be estimated as

$$\Delta\left(\frac{M_j}{\rho_j}\right) = \sqrt{\sum_{\text{for all } x} (\Phi_x \Delta x)^2} \tag{10}$$

where Φ_x is the sensitivity of molar volume to each of the measured parameters x (i.e., any of σ, ω, and υ_j)

$$\Phi_x = \frac{\partial}{\partial x}\left(\frac{M_j}{\rho_j}\right) \tag{11}$$

and Δx is the uncertainty in x. The Φ_x for Eq. (10) are obtained by differentiating Eq. (9) and are shown in Table 1.

2.5 Köhler theory analysis: inferring solubility

From Eq. (7), s_c for completely soluble CCN scales with $d^{-3/2}$. However, if an aerosol exhibits limited solubility, s_c will change its scaling dependence at a characteristic dry diameter, d^* (Fig. 1). This is because when $d<d^*$, the amount of water available at the point of activation is insufficient to dissolve all available solute (which gives a much steeper dependence of s_c vs. d). For $d>d^*$, all solute is dissolved and s_c scales with $d^{-3/2}$. Hence, $d=d^*$ corresponds to the solubility limit of the solute. Using Köhler theory, the solubility, C_{eq}, of the compound can be approximated as follows. The mass of dissolved solute, m, at the point of complete dissolution is:

$$m = \frac{\pi}{6}\varepsilon_s \rho_s d^{*3} \tag{12}$$

Table 1. Formulas used for computing the sensitivity of molar volume to σ, ω, and υ_j.

Property	Sensitivity, $\Phi_x = \frac{\partial}{\partial x}\left(\frac{M_j}{\rho_j}\right)$
σ	$\Phi_\sigma = \frac{768}{27}\left(\frac{M_w}{\rho_w}\right)^2\left(\frac{1}{RT}\right)^3\left(\frac{M_j}{\rho_j}\right)^2\frac{\sigma^2}{\varepsilon_j\upsilon_j\omega^2}$
ω	$\Phi_\omega = \frac{512}{27}\left(\frac{M_w}{\rho_w}\right)^2\left(\frac{1}{RT}\right)^3\left(\frac{M_j}{\rho_j}\right)^2\frac{\sigma^3}{\varepsilon_j\upsilon_j\omega^3}$
υ_j	$\Phi_{\upsilon_j} = -\frac{256}{27}\left(\frac{M_w}{\rho_w}\right)^2\left(\frac{1}{RT}\right)^3\left(\frac{M_j}{\rho_j}\right)^2\frac{\sigma^3}{\varepsilon_j\upsilon_j^2\omega^2} + \sum_{i\neq j}\left(\frac{M_j}{\rho_j}\right)^2\frac{\left(\frac{\rho_i}{M_i}\right)\varepsilon_i\upsilon_i}{\varepsilon_j\upsilon_j^2}$

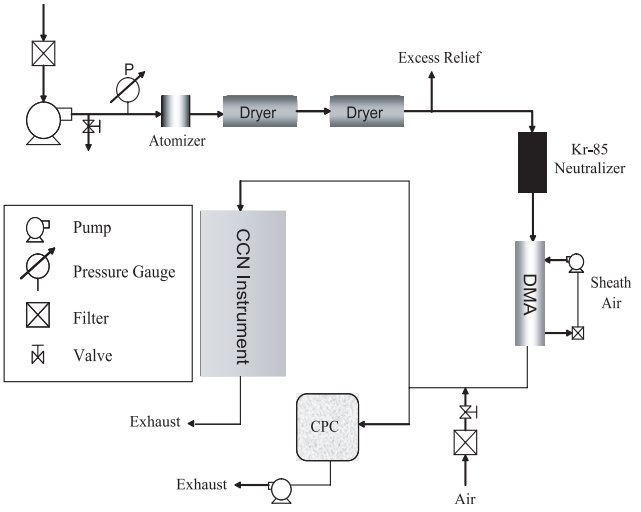

Fig. 2. Experimental setup used to measure CCN activity.

where ρ_s and ε_s is the density and volume fraction of solute, respectively. From Köhler theory, the droplet volume, V_d, at the critical diameter, D_c, is:

$$V_d = \frac{\pi}{6}D_c^3 = \frac{8}{27}\frac{\pi}{6}\frac{A^3}{s_c^{*3}} \tag{13}$$

where s_c^* is the critical supersaturation of the particle with dry diameter d^*. Assuming that V_d is approximately equal to the volume of water in the activated droplet, C_{eq} (in kg kg^{-1}) can be estimated as:

$$C_{eq} = \frac{m}{\rho_w V_d} \tag{14}$$

Introducing Eqs. (12) and (13) into (14) yields the solubility of the organic, C_{eq} (kg kg^{-1}),

$$C_{eq} = \frac{27}{8}\varepsilon_s\frac{\rho_s}{\rho_w}\frac{d^{*3}s_c^{*3}}{A^3} \tag{15}$$

3 Experimental procedure

3.1 Surface tension measurements

Surface tension is measured using a pendant drop tensiometer (CAM 200 Optical Contact Angle Meter, by KSV Inc.). A mechanically-controlled micro-syringe slowly drops the solution into a chamber where a snapshot of the droplet at the tip of a stainless steel needle is taken. The droplet shape is then fit to the Young-Laplace equation (Spelt and Li, 1996) from which the sample surface tension is obtained. Approximately seventy pictures (ten pictures per droplet) of seven different droplets (right before they fall off the tip of the needle) were taken in order to obtain averages and standard deviations for each solution. Carbon concentration was chosen as a basis for expressing surfactant concentration (Facchini et al., 1999b). Surface tension depression depends on the amount of dissolved carbon; therefore it is measured over a range of concentrations, starting at near the bulk solubility limit and then 1:2, 1:4, 1:8 dilutions with ultrafine pure water. Finally, one more "pure water" measurement was done corresponding to a "zero" carbon concentration solution, obtained by infinite dilution of the original sample. A plot of the solution surface tension, versus the water soluble organic carbon concentration (C_{WSOC}) was obtained for each inorganic/organic mixture and the data fitted to the Szyskowski-Langmuir equation (Langmuir, 1917),

$$\sigma = \sigma_w - \alpha T \ln(1 + \beta C_{\mathrm{WSOC}}) \tag{16}$$

where σ_w is the surface tension of water at temperature T and the parameters α and β are obtained by least squares minimization.

In order to introduce the measured surface tension into KTA, the conditions at the point of activation is determined for each supersaturation. Similar to Eq. (15), the average concentration of the organic at activation, C_{act}, is determined by:

$$C_{\mathrm{act}} = \frac{27}{8}\varepsilon_s\rho_s\frac{d^3 s_c^3}{A^3} \tag{17}$$

C_{act} is then substituted into Eq. (16) to obtain the surface tension at the point of activation.

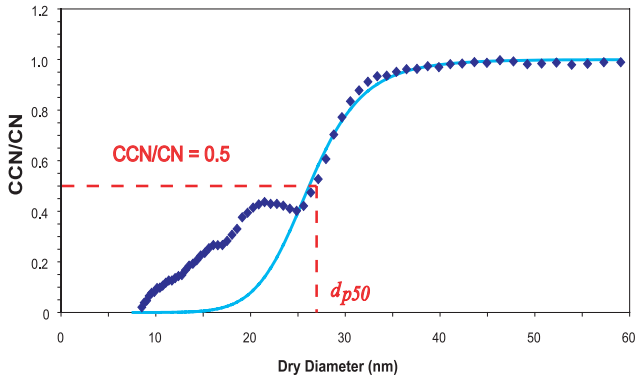

Fig. 3. Example of procedure used to determine d_{p50}. Shown are CCN/CN data obtained at 1.2% supersaturation for 50% malonic acid with its sigmoidal fit (light blue line). d_{p50} is the dry diameter for which CCN/CN=0.5.

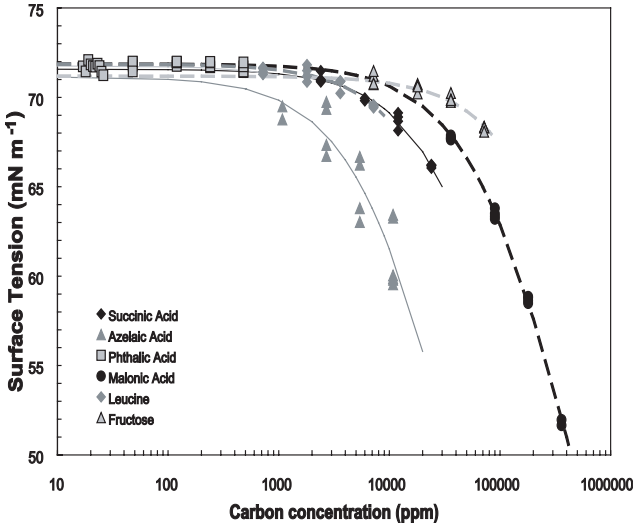

Fig. 4. Surface tension as a function of carbon concentration of mixed organic/inorganic aqueous solutions. Shown are succinic acid (black diamond), azelaic acid (grey triangle), phthalic acid (outlined grey square), malonic acid (black circle), leucine (grey diamond), and fructose (outlined grey triangle). The lines correspond to the Szyskowski-Langmuir fit for each organic.

3.2 CCN activity measurements

The setup used for measurement of CCN activity consists of three sections: aerosol generation, particle size selection, and CCN/CN measurement (Fig. 2). In the aerosol generation step, an aqueous solution of organic/inorganic is atomized with a controlled high velocity air stream atomizer. Compressed filtered air is introduced into the atomizer, the pressure of which controls the size distribution and flow rate of atomized droplets. A polydisperse aerosol is subsequently produced by drying the droplet stream by passing it through two silica-gel diffusional dryers.

The dry aerosol is then sent to the electrostatic classifier for particle size selection (TSI Model 3080) with a Differential Mobility Analyzer (DMA, TSI Model 3081). Before entering the classifier, the aerosols are passed through an impactor to remove supermicron particles; the remaining aerosol passes through a Kr-85 neutralizer which charges the particles. The particle size is then selected by a Differential Mobility Analyzer by allowing particles of the selected size (charge) to pass through producing a monodisperse aerosol. The monodisperse flow exiting the DMA at $1\,\mathrm{l\,min^{-1}}$ is mixed with filtered air and then sampled by a Condensation Particle Counter (CPC, TSI Model 3010) and a Continuous Flow Thermal Gradient Cloud Condensation Nuclei (CCN, DMT Inc.) Counter.

The CPC measures the total number concentration of condensation nuclei (CN) present for the specified aerosol size while the CCN counter counts the total number of particles that become activated as the aerosol is exposed to a constant water supersaturation. The CCN instrument operates by applying a linear temperature gradient across a wetted column; water vapor diffuses more quickly than heat, resulting in a constant water supersaturation along a streamline (Roberts and Nenes, 2005). CCN flowing about the column centerline activate and grow into cloud droplets ($D_p > 1\,\mu$m) and are counted at the exit with an optical particle counter (OPC). For our studies, particles ranging between 7 and 325 nm dry mobility diameters were selected and exposed to 0.2%, 0.4%, 0.6% and 1.2% supersaturation (SS) to obtain CCN activation curves (Fig. 3). The CCN instrument is calibrated daily with $(NH_4)_2SO_4$ to verify that it is operating properly.

Two approaches were applied to perform the particle size selection. In the first approach, called "stepping mode", the DMA voltage (i.e., monodisperse aerosol diameter) is constant for a period of time, during which the average CN and CCN concentrations are measured. This procedure is repeated over many particle sizes and CCN supersaturations. In the second approach, called Scanning Mobility CCN Analysis or SMCA (Nenes and Medina, 2007[1]), the DMA voltage is changed over time, so that the complete size range of dry particle size is "scanned" over 2 min. The time series of CN, CCN and voltage is then converted into activation curves using an inversion method (Nenes and Medina, 2007[1]). SMCA greatly reduces the time required for CCN activity measurements and the amount of sample required for its complete characterization.

CCN activity is characterized by the minimum dry particle diameter, d_{p50}, that activates at the supersaturation of interest. d_{p50} is found by plotting the ratio of CCN to CN concentration as a function of dry particle diameter and determining the dry diameter for which the CCN/CN ratio equals

[1]Nenes, A. and Medina, J.: Scanning Mobility CCN Analysis – A method for fast measurements of size resolved CCN activity and growth kinetics, Aerosol Sci. Technol., in review, 2007.

Table 2. Properties of compounds considered in this study. Organics are sorted in order of decreasing solubility.

Compound name	Chemical formula	Molar mass ($g\,mol^{-1}$)	Density ($g\,cm^{-3}$)	Solubility ($g/100\,g\ H_2O$)	Molar volume ($cm^3\,mol^{-1}$)	pKa[g]
Fructose	$C_6H_{12}O_6$	180.16	1.600[c]	407.4[c]	113	N/A
Malonic Acid	$C_3H_4O_4$	104.06	1.619[a]	154[d]	64	2.9 (5.7)
Succinic Acid	$C_4H_6O_4$	118.09	1.566[b]	8.76[b]	75	4.2 (5.6)
Leucine	$C_6H_{13}NO_2$	131.17	1.293[e]	2.3[e]	101	2.4 (5.98) (acid) 9.60 (amine)
Azelaic Acid	$C_9H_{16}O_4$	188.22	1.225[f]	0.2447[f]	154	N/A
Phthalic Acid	$C_8H_6O_4$	166.13	1.593[b]	0.1415[f]	104	2.9 (5.4)
Ammonium Sulfate	$(NH_4)_2SO_4$	132.14	1.77[d]	41.22[d]	75	

[a] Abbat et al. (2005).
[b] Hartz et al. (2006).
[c] Rosenørn et al. (2006).
[d] Material Safety Data Sheet.
[e] CRC Handbook (2002).
[f] Yaws' Handbook (2003).
[g] Solomons and Fryhle (2000).

0.50. To facilitate with the analysis, the data is fit to a sigmoid curve which then avoids considering the impact of multiply-charged particles (shown in Fig. 3 as a "hump" left to the sigmoid curve).

3.3 Compounds considered in this study

Table 2 summarizes the properties of the seven compounds (one inorganic salt and six organics) used in the experiments. Because of its atmospheric relevance, $(NH_4)_2SO_4$ was chosen as the inorganic salt. The organics include four carboxylic acids (succinic acid, azelaic acid, phthalic acid, and malonic acid), one amino acid (leucine), and one sugar (fructose). Succinic, azelaic, and malonic acids are dicarboxylic acids of varying chain length, while phthalic acid is a dicarboxylic acid with a benzene ring. Leucine is a branched six carbon amino acid with a carboxylic acid group and an amine group. Finally, fructose is a six carbon sugar that exists interchangeably between a chain and a 5-carbon ring structure. All of these compounds are representative of various biogenic and anthropogenic compounds found in atmospheric particles (Saxena and Hildemann, 1996), all with varying water solubility, carbon chain length, and surfactant characteristics.

For each organic compound, we characterized the surfactant properties and CCN activity for organic-$(NH_4)_2SO_4$ mixtures with the following organic/inorganic molar ratios: 100:0, 99:1, 95:5, 90:10, 50:50, 10:90, and 1:99. By varying the organic mass fraction, we assess the applicability of KTA over a wide range of organic/inorganic interaction strength. This is a particularly important test, as it will largely determine its applicability for complex mixtures typical of atmospheric aerosols. In applying KTA, we assume $\upsilon_j \sim 1$ for organics (e.g., Cruz and Pandis, 1997; Raymond and Pandis, 2002; Broekhuizen et al., 2004; Abbatt et al., 2005; Hartz et al., 2006) and $\upsilon_j \sim 2.5$ for $(NH_4)_2SO_4$ (e.g., Brechtel and Kreidenweis, 2000). Finally, we quantify the uncertainty of the inferred molar volume from uncertainties in σ, ω, υ_j for all mixtures considered.

4 Results

4.1 Surface tension measurements

Surface tension was measured for all pure organic and mixtures with $(NH_4)_2SO_4$ as a function of C_{WSOC}; the data was subsequently fit to the Szyskowski-Langmuir equation for use in KTA. Figure 4 shows the surface tension dependence of C_{WSOC} for all organic species (high organic fraction) each fitted to the Szyskowski-Langmuir equation. All compounds were found to depress surface tension except for phthalic acid in the range of concentration studied. The strongest surface active compounds were malonic acid and azelaic acid; fructose, leucine and succinic acid showed moderate surfactant behavior in the range of concentrations considered.

To address the effects of salts in the surfactant behavior of organics, we compared the surface tension depression of each organic when dissolved in water alone and mixed with $(NH_4)_2SO_4$. Examples of the surface tension dependence of pure succinic acid and mixtures with $(NH_4)_2SO_4$ are shown in Fig. 5a (high organic fractions) and Fig. 5b (low organic fractions). Adding small amounts of $(NH_4)_2SO_4$ does not affect the surfactant behavior of succinic acid at high organic fractions (Fig. 5a). At low organic concentrations, introduction of greater amounts of $(NH_4)_2SO_4$ to the succinic acid

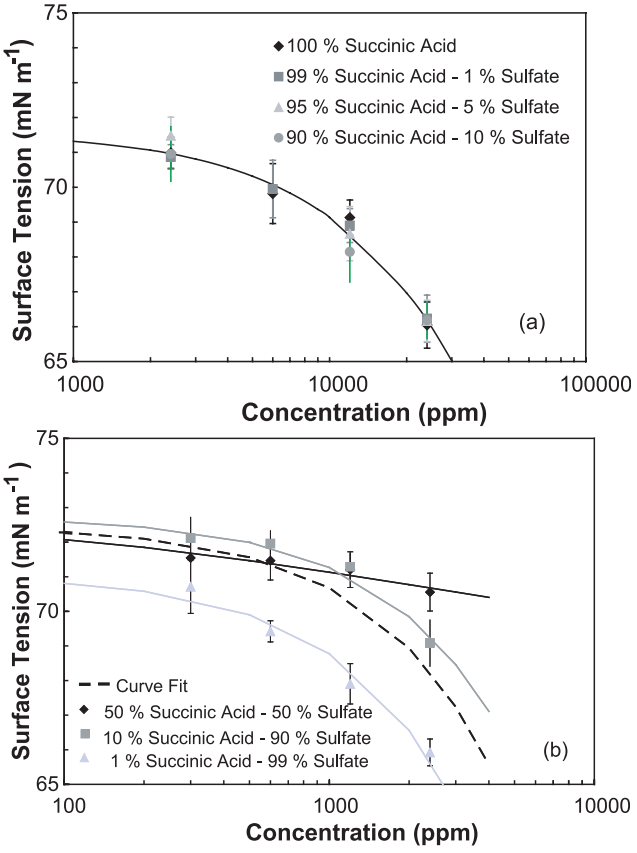

Fig. 5. (a) Surface tension as a function of carbon concentration for pure succinic acid (black diamond) and mixtures with $(NH_4)_2SO_4$ for 99% (grey square), 95% (grey triangle), and 90% (grey circle) succinic acid (mol fraction). The solid black line corresponds to the Szyskowski-Langmuir fit for all high organic fraction mixtures. **(b)** Surface tension depression as a function of carbon concentration for $(NH_4)_2SO_4$ – succinic acid mixtures for 50% (black diamond), 10% (grey square), and 1% (grey triangle) succinic acid (mol fraction). The solid lines correspond to the Szyskowski-Langmuir fit for each mixture: 50% (black line), 10% (dark grey line), and 1% (light grey line). The dashed black line corresponds to the Szyskowski-Langmuir fit for all three low organic fraction mixtures.

solution can further decrease the surface tension beyond that of the pure organic (Fig. 5b). As an example, for a C_{WSOC} of 2000 ppm, the surface tension for pure succinic acid (100%) is 71 mN m^{-1} while for a 1% succinic acid solution, at the same concentration, the surface tension is depressed down to 66.5 mN m^{-1}. The observed decrease in surface tension with salt concentration increase could be explained by the interaction between ammonium sulfate and organic molecules. The presence of the inorganic electrolyte at high concentrations forces the "organic" to partition to the surface creating a surfactant rich layer; this "salting out" effect decreases the surface tension beyond that of the pure organic component (Kiss et al., 2005).

Table 3. Szyskowski-Langmuir constants (298 K) for computing the surface tension of aqueous organic solutions. The same parameters apply for pure organic solutions and mixtures with $(NH_4)_2SO_4$ (up to 10% salt mol fraction). C_{max} is the maximum concentration of organic used in the measurements.

Compound	$\alpha \times 10^1$ (mN m^{-1} K^{-1})	$\beta \times 10^5$ (ppm^{-1})	$C_{max} \times 10^{-3}$ (ppm)
Fructose	1.896	0.0709	180
Malonic Acid	0.434	1.0039	1040
Succinic Acid	0.652	1.3383	59
Leucine	1.947	0.5702	13
Azelaic Acid	0.484	9.4885	1.9
Phthalic Acid	1.930	0.9170	0.831

Table 4. Szyskowski-Langmuir constants (298 K) for computing the surface tension of aqueous organic solutions mixed with $(NH_4)_2SO_4$ for larger than 10% salt mole fraction.

Compound	Organic Mole Fraction (%)	$\alpha \times 10^1$ (mN m^{-1} K^{-1})	$\beta \times 10^5$ (ppm^{-1})
Malonic Acid	50	5.3316	1.381
	10	5.3316	1.381
	1	0.5000	1.946
Succinic Acid	50	0.0185	1004
	10	1.8031	2.756
	1	3.4842	2.202
Azelaic Acid	50	0.2045	454.4
	10	21.322	2.404
	1	23.917	3.012

Since the addition of $(NH_4)_2SO_4$ did not substantially affect the droplet surface tension for the high organic fraction solutions considered (90%–100%), all molar fraction solutions of each species were fit to Eq. (16) in order to obtain average α and β parameters (Table 3), which subsequently can be introduced to KTA. For low organic fractions (50%, 10%, and 1%), $(NH_4)_2SO_4$ has an important impact on surface tension, so α and β must be determined at each sulfate concentration (Table 4; Fig. 5b).

4.2 CCN measurements

Activation curves for pure succinic acid and mixtures with $(NH_4)_2SO_4$ are shown in Fig. 6. As the organic mass fraction decreases from 100% to 50%, the activation curves of the mixtures move towards the $(NH_4)_2SO_4$ curve. Therefore, small amounts of salt present notably impact the CCN activity of the organic material. On the other hand, when small amounts of organics are introduced to a $(NH_4)_2SO_4$ particle, the aerosol has a higher CCN activity than pure $(NH_4)_2SO_4$;

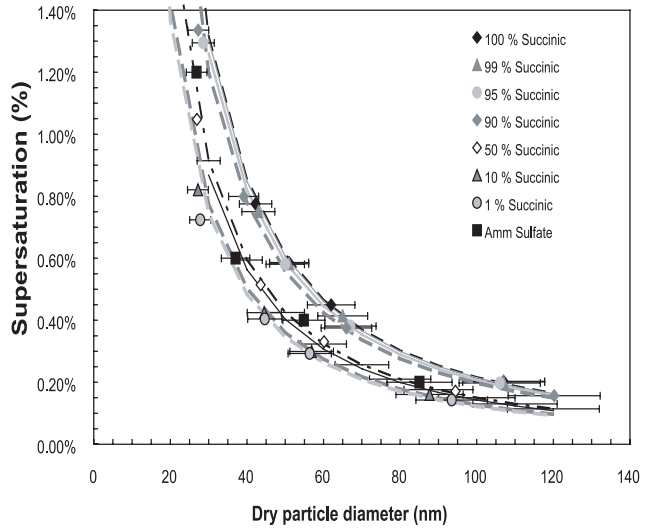

Fig. 6. Activation curves for pure succinic acid (black diamond) and mixtures with $(NH_4)_2SO_4$ consisting of 99% (grey triangle), 95% (grey circle), 90% (grey diamond), 50% (open diamond), 10% (outlined grey triangle), and 1% (outlined grey circle) molar fraction of succinic acid. Activation curve for $(NH_4)_2SO_4$ (black square) is also plotted for comparison. The solid and dash lines (100% (black dash line), 99% (dark grey line), 95% (light grey line), 90% (dark grey dashed line), 50% (black dash dot line), 10% (dashed dark grey), 1% (dashed light grey) and $(NH_4)_2SO_4$ (black line)) indicates a power fit to the data.

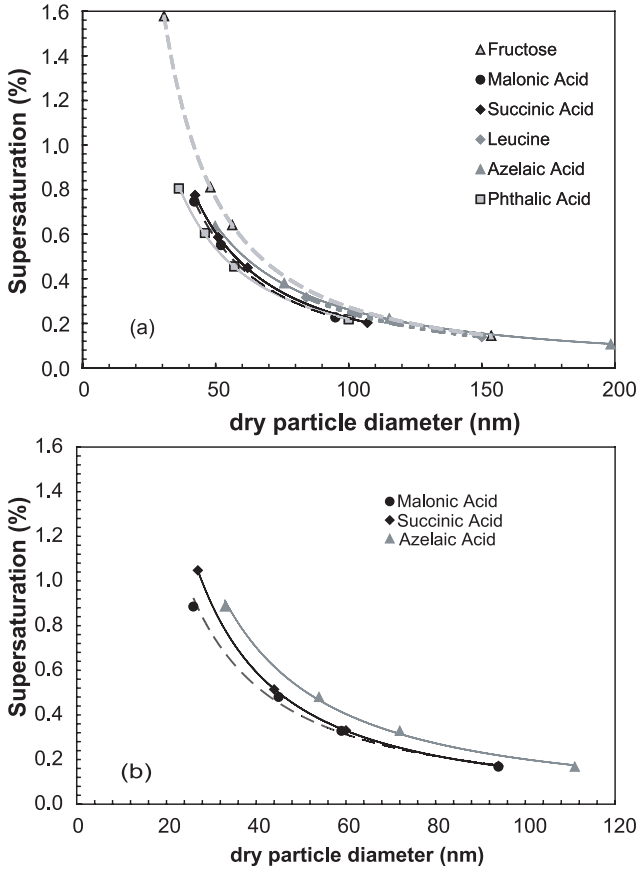

Fig. 7. (a) Activation curves for pure organic components: succinic acid (black diamond), azelaic acid (grey triangle), phthalic acid (outlined grey square), malonic acid (black circle), leucine (grey diamond), and fructose (outlined grey triangle). The lines correspond to a power law fit to the activation data. **(b)** Activation curves for 50% organic fraction mixtures with $(NH_4)_2SO_4$: azelaic acid (grey triangle), phthalic acid (outlined grey square), and malonic acid. The lines correspond to a power law fit to the activation data.

the surface tension depression from the presence of organics allows the droplet activation to occur at lower supersaturations. The same behavior was observed for all mixtures.

Comparison of CCN activity (activation curves) are presented in Figs. 7a and b for organic aerosol mixed with $(NH_4)_2SO_4$. The observed CCN activity was not consistent with solubility reported in Table 2; in fact, all cases studied behaved as if they were completely soluble, possibly because of aerosol metastability or the effect of curvature-enhanced solubility (Padró and Nenes, 2007). As the measurements suggest that most compounds studied are not strong surfactants (Fig. 4), we expect CCN activity to correlate with the number of moles at the point of activation, i.e., the effective van't Hoff factor (the moles of ions released per mol of solute) over the molar volume. Thus, phthalic acid should produce better CCN than fructose; the two have comparable molar volumes (Table 2) but the carboxyl groups in phthalic acid dissociate substantially (low pKa, i.e. van't Hoff factor >1), while fructose does not dissociate at all (i.e. van't Hoff factor =1). Using this approach, one can rank the compounds in terms of decreasing CCN activity as follows: ammonium sulfate, phthalic acid, malonic acid, succinic acid, leucine, azelaic acid, and fructose. Our measurements support this ranking.

The high CCN activity of leucine in our study is in disagreement with other published data (e.g., Hartz el al., 2006). We attribute this difference to the phase state of the aerosol introduced in the CCN instrument: our atomized particles were "softly" dried down to $\sim$10% RH (as measured using a RH probe inline); under such conditions aerosol tends to retain water (Padró and Nenes, 2007) and leucine does not crystallize out of solution. In contrast, other studies used more aggressive drying methods (for example, Hartz el al., 2006, used a silica gel followed by an activated carbon dryer) which likely resulted in much drier leucine particles.

4.3 Evaluation of inferred molar volumes

Köhler theory analysis requires knowledge of the parameters α, β (Tables 3 and 4), and ω (Table 5), which are introduced

Table 5. Results of Köhler theory analysis for the compounds and mixtures considered in this study. Organics are arranged in order of decreasing solubility.

Compound (Molar Volume)	Organic Mole Fraction (%)	$\omega \times 10^{14}$ ($m^{3/2}$)	Inferred Molar Volume ($cm^3\,mol^{-1}$)	Molar Volume Error (%)
Fructose	100	8.478	112.868	0.2
($113\,cm^3\,mol^{-1}$)	99	8.527	115.207	2
	95	8.075	111.447	1
	90	7.587	106.600	5
Malonic Acid	100	6.473	66.150	3
($64\,cm^3\,mol^{-1}$)	99	6.398	65.089	1
	95	6.195	63.531	1
	90	5.944	62.145	3
	50	4.588	68.328	6
	10	3.965	3.082	95
	1	3.904	0.016	100
Succinic Acid	100	6.839	89.368	19
($75\,cm^3\,mol^{-1}$)	99	6.777	88.680	18
	95	6.548	81.394	8
	90	6.227	76.909	2
	50	4.753	58.130	23
	10	4.024	7.313	90
	1	3.863	0.099	100
Leucine	100	7.807	139.106	37
($101\,cm^3\,mol^{-1}$)	99	7.960	183.440	81
	95	7.435	125.739	24
	90	7.054	113.670	12
Azelaic Acid	100	8.146	281.794	83
($154\,cm^3\,mol^{-1}$)	99	7.867	190.044	23
	95	7.062	135.549	12
	90	6.804	131.878	14
	50	3.986	212.967	38
	10	2.462	161.931	5
	1	4.099	691.836	349
Phthalic Acid	100	5.787	90.024	14
($104\,cm^3\,mol^{-1}$)	99	5.605	82.449	21
	95	5.617	89.298	14
	90	5.630	107.624	3

into Eq. (9). The calculated $\left(\frac{M_j}{\rho_j}\right)$ as well as its error with respect to expected values are shown in Table 5. Predicted molar volume of each organic was closest to literature values when the organic mass fraction is 50% and above; under such conditions, the average error in inferred molar volume was found to be 18%. In terms of the molar volume error dependence with organic fraction (Table 5), two types of patters are seen: i) for the soluble non-surfactant compounds (fructose, malonic acid) error is almost zero for pure compound and increases as the organic mass fraction decreases, ii) for sparingly-soluble and surface-active species (leucine, phthalic acid, succinic acid and azelaic acid), errors tends to be larger when (almost) pure compound is activated, reaches a minimum at the 90–50% organic fraction range, and then increases again at lower organic factions. In both pattern types, the error at small organic fractions is consistent with the expectation that molar volume uncertainty is inversely proportional to organic fraction (Eq. 10, Table 1). In pattern type (ii), the simple form of Köhler theory used when applying KTA (Eqs. 1–4) does not consider the effect of surface layer partitioning on critical supersaturation (Sorjamaa et al., 2004; Sorjamaa and Laaksonen, 2006); this may introduce a bias in inferred molar volume which becomes maximum when the organic mass fraction is high. Furthermore, since surfactants are not very soluble (Table 2), they may not completely dissolve at the point of activation (when they constitute most of the CCN dry mass), which leads to an overestimation of solute molar volume (Table 5). Addition of some deliquescent material (ammonium sulfate) enhances the amount of water in the CCN and facilitates

Table 6. Molar volume uncertainty analysis and total uncertainty as percent of molar volume for the compounds and mixtures considered in this study.

Compound	Organic Mole Fraction (%)	Uncertainty to σ ($cm^3\,mol^{-1}$)	Uncertainty to ω ($cm^3\,mol^{-1}$)	Uncertainty to υ_{org} ($cm^3\,mol^{-1}$)	Total Uncertainty ($cm^3\,mol^{-1}$)	Total Uncertainty (%)
Fructose	100	0.192	16.166	22.453	38.811	34.3
	99	0.250	16.227	22.537	39.014	34.5
	95	0.246	18.789	26.095	45.130	40.0
	90	0.241	22.588	31.372	54.200	48.0
Malonic	100	0.064	6.641	9.224	15.802	24.7
Acid	99	0.058	6.909	9.596	16.448	25.7
	95	0.037	7.764	10.783	18.510	28.9
	90	0.064	8.937	12.412	21.285	33.3
	50	0.222	14.479	31.807	46.064	72.0
	10	0.821	215.477	169.300	383.956	599.9
	1	14.756	2620.228	2600.989	5206.452	8135.1
Succinic	100	0.103	8.046	12.572	20.515	27.4
Acid	99	0.106	8.265	12.915	21.074	28.1
	95	0.126	10.043	15.692	25.608	34.1
	90	0.170	12.424	19.413	31.668	42.2
	50	0.364	52.018	59.111	110.765	147.7
	10	2.569	124.850	346.807	469.089	625.5
	1	28.494	2787.770	3871.907	6631.177	8841.6
Leucine	100	0.138	8.529	11.846	20.237	20.0
	99	0.093	6.337	8.801	15.044	14.9
	95	0.130	11.045	15.341	26.257	26.0
	90	0.224	14.998	20.830	35.604	35.3
Azelaic	100	0.227	13.847	18.219	31.839	20.7
Acid	99	0.258	18.859	24.814	43.414	28.2
	95	0.479	27.903	36.714	64.138	41.6
	90	0.453	35.492	46.700	81.738	53.1
	50	0.951	50.995	106.240	156.284	101.5
	10	7.624	490.647	721.541	1204.567	782.2
	1	70.198	13 308.622	12 322.813	25 561.27	16 598.2
Phthalic	100	0.436	40.802	56.669	97.907	94.1
Acid	99	0.427	45.036	62.549	108.007	103.9
	95	0.435	46.667	64.813	111.913	107.6
	90	0.471	51.794	71.936	124.201	119.4

complete dissolution of the organic fraction (which can be further enhanced from curvature-enhanced solubility, Padró and Nenes, 2007). As a result, the inferred molar volume error decreases as s_c more closely scales with $d^{-3/2}$. When the organic fraction is low (<50%), the CCN at the point of activation becomes concentrated in ammonium sulfate and the organic may "salt out" (i.e., precipitate out of solution). This affects the solution surface tension and number of dissolved moles, which eventually increases the error in molar volume (Table 5). Phthalic acid is in less error compared to leucine and azelaic acid (despite the "bulk" solubility of the former being lower than the latter two), likely because it is the least surface-active of the type (ii) compounds, hence least subject to surface-partitioning effects. Overall, the assumption of complete solubility used in KTA seems to work well, particularly for cases where organics are mixed with some sulfate.

Estimating average molar volume uncertainty requires computing its sensitivity with respect to σ, ω , υ_j and the estimated uncertainty in those parameters (Table 6). Of the three parameters, ω and υ_j were found to introduce the greatest uncertainty; while the uncertainty in σ is rather small. The greater uncertainty (∼55%) for all the compounds arises from the van't Hoff factor (dissociation in water). The uncertainty in this parameter is high since we assumed υ_j=1 when in reality it is larger (since most of the dicarboxylic acids we studied dissociate, pKa<3). Error estimates increase as the organic fraction decreases, since the sensitivities, Φ_x, depend inversely on the organic mass fraction (Table 1).

From our assessment of KTA, the new method applies best for relatively high organic mass fractions but with some deliquescent material to insure sufficient water uptake for complete dissolution of constituents. It is suggested that the method should not be used for the low organic fraction aerosols because: *i*) salting out effects can become very important and *ii)* the sensitivities scale with ε_j^{-1} and uncertainties are magnified substantially for volume fractions below 20 %. The uncertainty estimated from Eq. (10) (Table 6) is usually larger than the actual molar volume (Table 5), which suggests that Eq. (10) can be used as an upper limit estimate.

5 Conclusions

This study presents a new method, Köhler Theory Analysis, to infer the molar volume, solubility, and surfactant characteristics of water soluble atmospheric organic matter. This is done by combining Köhler theory with measurements of surface tension, chemical composition, and CCN activity. In addition to presenting KTA, we evaluate the method by comparing inferred molar volumes to their expected values for particles composed of six organics (azelaic acid, malonic acid, phthalic acid, succinic acid, leucine, and fructose) in pure form or mixed with $(NH_4)_2SO_4$. CCN activation experiments were done at 0.2%, 0.4%, 0.6%, and 1.2% supersaturation.

Köhler theory analysis was found to predict the average error in molar volume to within 18% of the expected value when the organic mass fraction ranges between 50 and 90%. The estimated molar volume error was found to be larger than its actual value (most likely from surface partitioning and partial solubility effects). KTA is a potentially powerful tool for characterizing the droplet formation potential of ambient water soluble organic carbon, as it can provide much needed constraints for physically-based assessments of the aerosol indirect effect.

Acknowledgements. This research was supported by a NSF CAREER Award, NASA Headquarters under the Earth System Science Fellowship Grant and another NASA Proposal (NNG04GE16G). We also thank A. Laaksonen and 3 anonymous reviewers for comments that substantially improved the manuscript.

Edited by: W. E. Asher

References

CRC: Handbook of Chemistry and Physics, Ed., CRC Press, New York, 2002.

Abbatt, J. P. D., Broekhuizen, K., and Kumal, P. P.: Cloud condensation nucleus activity of internally mixed ammonium sulfate/organic acid aerosol particles, Atmos. Environ., 39(26), 4767–4778, 2005.

Albrecht, B. A.: Aerosols, cloud microphysics, and fractional cloudiness, Science, 245, 1227–1230, 1989.

Bilde, M. and Svenningsson, B.: CCN activation of slightly soluble organics: the importance of small amounts of inorganic salt and particle phase, Tellus Series B-Chemical and Physical Meteorology, 56(2), 128–134, 2004.

Bretchel, F. J. and Kreidenweis, S. M.: Predicting particle critical supersaturation from hygroscopic growth measurements in the humidified TDMA. Part I: Theory and sensitivity studies, J. Atmos. Sci., 57(12), 1854–1871, 2000.

Broekhuizen, K., Kumar, P. P., and Abbatt, J. P. D.: Partially soluble organics as cloud condensation nuclei: Role of trace soluble and surface active species, Geophys. Res. Lett., 31(1), L01107, doi:10.1029/2003GL018203, 2004.

Broekhuizen, K., Chang, R. Y.-W., Leaitch, W. R., Li, S.-M., and Abbatt, J. P. D.: Closure between measured and modeled cloud condensation nuclei (CCN) using size-resolved aerosol compositions in downtown Toronto, Atmos. Chem. Phys., 6, 2513–2524, 2006, http://www.atmos-chem-phys.net/6/2513/2006/.

Cruz, C. N. and Pandis, S. N.: A study of the ability of pure secondary organic aerosol to act as cloud condensation nuclei, Atmos. Environ., 31(15), 2205–2214, 1997.

Decesari, S., Facchini, M. C., Fuzzi, S., and Tagliavini, E.: Characterization of water-soluble organic compounds in atmospheric aerosol: A new approach, J. Geophys. Res.-A., 105(D1), 1481–1489, 2000.

Facchini, M. C., Decesari, S., Mircea, M., Fuzzi, S., and Loglio, G.: Surface tension of atmospheric wet aerosol and cloud/fog droplets in relation to their organic carbon content and chemical composition, Atmos. Environ., 34(28), 4853–4857, 2000.

Facchini, M. C., Fuzzi, S., Zappoli, S., Andracchio, A., Gelencser, A., Kiss, G., Krivacsy, Z., Meszaros, E., Hansson, H. C., Alsberg, T., and Zebuhr, Y.: Partitioning of the organic aerosol component between fog droplets and interstitial air, J. Geophys. Res.-A., 104(D21), 26 821–26 832, 1999a.

Facchini, M. C., Mircea, M., Fuzzi, S., and Charlson, R. J.: Cloud albedo enhancement by surface-active organic solutes in growing droplets, Nature, 401(6750), 257–259, 1999b.

Feingold, G. and Chuang, P. Y.: Analysis of the influence of film-forming compounds on droplet growth: Implications for cloud microphysical processes and climate, J. Atmos. Sci., 59(12), 2006–2018, 2002.

Giebl, H., Berner, A., Reischl, G., Puxbaum, H., Kasper-Giebl, A., and Hitzenberger, R.: CCN activation of oxalic and malonic acid test aerosols with the University of Vienna cloud condensation nuclei counter, J. Aerosol Sci., 33(12), 1623–1634, 2002.

Hartz, K. E. H., Tischuk, J. E., Chan, M. N., Chan, C. K., Donahue, N. M., and Pandis, S. N.: Cloud condensation nuclei activation of limited solubility organic aerosol, Atmos. Environ., 40(4), 605–617, 2006.

IPCC, Climate Change (2001): The Scientific Basis, Ed., Cambridge University Press. United Kingdom, 2001.

Kanakidou, M., Seinfeld, J. H., Pandis, S. N., Barnes, I., Dentener, F. J., Facchini, M. C., Van Dingenen, R., Ervens, B., Nenes, A., Nielsen, C. J., Swietlicki, E., Putaud, J. P., Balkanski, Y., Fuzzi, S., Horth, J., Moortgat, G. K., Winterhalter, R., Myhre, C. E. L., Tsigaridis, K., Vignati, E., Stephanou, E. G., and Wilson, J.: Organic aerosol and global climate modelling: a review, Atmos. Chem. Phys., 5, 1053–1123, 2005, http://www.atmos-chem-phys.net/5/1053/2005/.

Kiss, G., Tombacz, E., and Hansson, H. C.: Surface tension effects of humic-like substances in the aqueous extract of tropospheric fine aerosol, J. Atmos. Chem., 50(3), 279–294, 2005.

Köhler, H.: The nucleus in and the growth of hygroscopic droplets, Transactions of the Faraday Society, 32(2), 1152–1161, 1936.

Kumar, P. P., Broekhuizen, K., and Abbatt, J. P. D.: Organic acids as cloud condensation nuclei: Laboratory studies of highly soluble and insoluble species, Atmos. Chem. Phys., 3, 509–520, 2003, http://www.atmos-chem-phys.net/3/509/2003/.

Langmuir, I.: The constitution and fundamental properties of solids and liquids. II. Liquids., J. Am. Chem. Soc., 39, 1848–1906, 1917.

Nenes, A., Charlson, R. J., Facchini, M. C., Kulmala, M., Laaksonen, A., and Seinfeld, J. H.: Can chemical effects on cloud droplet number rival the first indirect effect?, Geophys. Res. Lett., 29(17), 1848, doi:10.1029/2002GL015295, 2002.

Padró, L. T. and Nenes, A.: Cloud droplet activation: solubility revisited, Atmos. Chem. Phys. Discuss., 7, 2325–2355, 2007, http://www.atmos-chem-phys-discuss.net/7/2325/2007/.

Raymond, T. M. and Pandis, S. N.: Cloud activation of single-component organic aerosol particles, J. Geophys. Res.-A., 107(D24), 4787, doi:10.1029/2002JD002159, 2002.

Raymond, T. M. and Pandis, S. N.: Formation of cloud droplets by multicomponent organic particles, J. Geophys. Res.-A., 108(D15), 4469, doi:10.1029/2003JD003503, 2003.

Roberts, G. C. and Nenes, A.: A continuous-flow streamwise thermal-gradient CCN chamber for atmospheric measurements, Aerosol Sci. Technol., 39(3), 206–211, 2005.

Rosenørn, T., Kiss, G., and Bilde, M.: Cloud droplet activation of saccharides and levoglucosan particles, Atmos. Environ., 40(10), 1794–1802, 2006.

Saxena, P. and Hildemann, L. M.: Water-soluble organics in atmospheric particles: A critical review of the literature and application of thermodynamics to identify candidate compounds, J. Atmos. Chem., 24(1), 57–109, 1996.

Seinfeld, J. H. and Pandis, S.: Atmospheric Chemistry and Physics, Ed., John Wiley, New York, 1998.

Shulman, M. L., Jacobson, M. C., Carlson, R. J., Synovec, R. E., and Young, T. E.: Dissolution behavior and surface tension effects of organic compounds in nucleating cloud droplets, Geophys. Res. Lett., 23(3), 277–280, 1996.

Solomons, G. and Fryhle, C.: Organic Chemistry, Ed., John Wiley & Sons, Inc., New York, 2000.

Sorjamaa, R. and Laaksonen, A.: The influence of surfactant properties on critical supersaturations of cloud condensation nuclei, J. Aerosol Sci., 37(12), 1730–1736, 2006.

Sorjamaa, R., Svenningsson, B., Raatikainen, T., Henning, S., Bilde, M., and Laaksonen, A.: The role of surfactants in Köhler theory reconsidered, Atmos. Chem. Phys., 4, 2107–2117, 2004, http://www.atmos-chem-phys.net/4/2107/2004/.

Spelt, J. K. and Li, D.: Applied Surface Thermodynamics, Ed., Marcel Dekker, Inc., New York, 1996.

Sullivan, A. P. and Weber, R. J.: Chemical characterization of the ambient organic aerosol soluble in water: 1. Isolation of hydrophobic and hydrophilic fractions with a XAD-8 resin, J. Geophys. Res.-A., 111(D5), D05314, doi:10.1029/2005JD006485, 2006a.

Sullivan, A. P. and Weber, R. J.: Chemical characterization of the ambient organic aerosol soluble in water: 2. Isolation of acid, neutral, and basic fractions by modified size-exclusion chromatography, J. Geophys. Res.-A., 111(D5), D05315, doi:10.1029/2005JD006486, 2006b.

Twomey, S.: Minimum size of particle for nucleation in clouds, J. Atmos. Sci., 34(11), 1832–1835, 1977.

Yaws, C. L.: Yaw's handbook of thermodynamic and physical properties of chemical compounds, Ed., Knovel, New York, 2003.

Zappoli, S., Andracchio, A., Fuzzi, S., Facchini, M. C., Gelencser, A., Kiss, G., Krivacsy, Z., Molnar, A., Meszaros, E., Hansson, H. C., Rosman, K., and Zebuhr, Y.: Inorganic, organic and macromolecular components of fine aerosol in different areas of Europe in relation to their water solubility, Atmos. Environ., 33(17), 2733–2743, 1999.